Morphable Components Topology Optimization for Additive Manufacturing

Y. Xian, and D. W. Rosen*

George W. Woodruff School of Mechanical Engineering, Georgia Institute of Technology, Atlanta, GA 30332

* Corresponding author. Email: david.rosen@me.gatech.edu

Abstract

This paper addresses two issues: 1. Topology optimization (TO) yields designs that may require support structures if additively manufactured, which increase material and clean-up costs. 2. Material anisotropy is induced during additive manufacturing, which results in inaccurate TO results if such material properties are not included in the algorithm. This paper, based on a moving morphable components (MMC) approach where structure is composed of several building blocks, introduces constraints for minimum build angle, as well as a penalty constraint for building blocks with no support material below, so that the TO output is completely printable. Additionally, orthotropic material properties are integrated in the optimization. In a separate optimization algorithm, each building block is assumed to have its own fiber orientation.

Introduction

Additive manufacturing (AM) refers to processes in which 3D objects are built layer by layer under computer control. Compared to traditional manufacturing processes, where material is "subtracted" from a block of material, AM fabricates highly complex parts more easily.

Topology optimization (TO) redistributes material in a design space, by providing sensitivity analysis to an optimization algorithm. After the topology optimization, the structure usually needs to go through a series of post-processing, for example, smoothing and/or a subsequent shape optimization, because topology optimization results usually cannot be used as is for design purposes.

There is significant interest today in integrating additive manufacturing and topology optimization, for several reasons, a major one being that topology optimization puts material only where it's needed, which produces light-weight results that help save weight a great deal in AM. Weight saving is a benefit during the product's useful life. For example, weight savings for a part in an aircraft can save thousands of gallons of fuel, millions of dollars, and greatly reduce pollution. Secondly, topologically optimized designs are geometrically complex, which are hard to manufacture using traditional processes, but could often be easily additively manufactured.

Though AM gives much freedom in the designs, making proper use of topology optimization to render additively manufacturable designs remains a challenging and vibrant research area for the past decade.

One of the most common challenges to additively manufacture certain TO structures is building designs with overhangs requires support structures, which directly increase build time and material cost; and machines have minimum allowable feature size limitations which TO results may not meet. Also, topologically optimized designs often consist of discretized geometry and implicit boundary, which makes subsequent design difficult due to the lack of parametric surfaces and dimensions. Another issue we want to address in this work is that, due to the layer by layer nature of most 3D printing processes, the printed parts would exhibit anisotropic material properties, where they frequently fail more easily when loaded along the build direction due to weak interlayer bonding.

Driven by the above challenges, we propose an optimization method based on a moving morphable component model developed by Dr. Xu Guo's research group from Dalian University of Technology in China. This approach uses explicit level set method for boundary representation, but at the same time its concept is similar to density-based method.

The proposed TO method represents the optimized structure using parameterized structural components. Hence, the TO result is a geometric model with explicit boundary elements that is readily importable into mechanical CAD systems for subsequent design and engineering work. A second objective is to remove overhangs from the designs. A third objective is to take into account 2D orthotropic material properties.

Literature Review

Topology optimization

In the literature, one can find a multitude of approaches for solving topology optimization problems. The following is a brief review of some of the key approaches.

One popular approach called homogenization method was firstly proposed by Bendsøe and Kikuchi (1988) [1]. The main idea of the homogenization method is to introduce periodically distributed micro-scale voids in a given homogeneous material. The effective material properties of the composite are then computed using homogenization theory. In this way, the material layout problem could be treated as an easier sizing problem, the sizing variable being the density of the perforated composite (i.e. sizes of holes). However, homogenization method often produces designs with infinitesimal pores that make the structure non-manufacturable.

One variation of the homogenization method later investigated was the SIMP approach (Solid Isotropic Material with Penalization), firstly by Bendsøe (1989) [2]. In SIMP, elements' relative densities are the design variables, which could be updated using several updating schemes, such as OC (Optimality Criteria), SLP (Sequential Linear Programming) methods, and MMA (Method of Moving Asymptotes). To penalize the intermediate densities, material properties are modeled to be proportional to the relative density raised to some power [3].

An alternative class of methods to the above density-based approaches is the boundary-based methods for structural optimization [4], a major approach of which is to use level set method to represent implicit, moving boundaries for topology optimization.

The level set method was first used by Osher and Sethian (1988) [5] as a method to implicitly represent the moving interfaces. In such analyses, the equations of motion of propagating fronts were approximated by the Hamilton-Jacobi equation. It was later applied in topology optimization to track the structural boundary, using an appropriate velocity normal to the boundary interface. Design variables are usually level set function values at the nodes.

MMC

With the aim of doing topology optimization in a more explicit and geometrical manner, a so-called moving morphable components (MMC) based topology optimization framework, which is quite different from the existing ones, was established by Guo (2014) [6]. The distinctive feature of this approach is that a set of morphable components are used as building blocks of topology optimization and the optimal structural topologies are found by optimizing the shapes, lengths, thicknesses, orientations and layout (connectivity) of these components.

Overhang Angle Constraints

Each 3D printer has its minimum build angle as one of its machine specifications. If part of a structure has an angle (with horizontal plane) below the minimum build angle, the structure would not be printed without support material.

To integrate AM-specific manufacturing constraints into optimization formulations, we added angle constraints into the original moving morphable components approach. More specifically, these angle constraints ensure that the centerline (i.e. local x-axis) of each building block forms an angle (with the print plane) that is larger or equal to the predefined minimum build angle.

The problem formulation is as follows:

- For a building block k, the design vector is: $\boldsymbol{D}_k = (x_{0k},\ y_{0k},\ L_k,\ t_k^1,\ t_k^2,\ t_k^3,\ st_k)$. $st_k \equiv sin\theta_k$.
- Find $\boldsymbol{D} = (\boldsymbol{D}_1, .., \boldsymbol{D}_n)$
- Minimize $C = f^T U$
- Such that $\int H\big(\phi^s(x; \boldsymbol{D})\big) dV \leq \bar{V}$ (volume constraint),
- and $f_k(x) = (sin\bar{\theta})^2 - (sin\theta_k)^2 \leq 0, k = 1,2, \ldots n$ (angle constraints).
- $\bar{V},\ \bar{\theta}$ are the maximum volume fraction and minimum build angle prescribed by designer.

Each building block has seven design variables, $\boldsymbol{D}_k = (x_{0k},\ y_{0k},\ L_k,\ t_k^1,\ t_k^2,\ t_k^3,\ sin\theta_k)$, [7]: block center, half length, 3 half thicknesses, and block orientation. As illustrated in Figure 1, each block is completely parameterized by the variables.

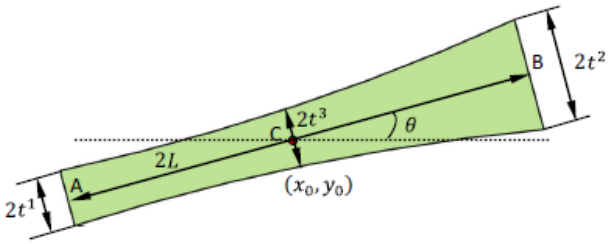

Fig 1. A building block is parameterized with seven design variables.

An angle constraint is imposed upon each building block [8]. Sensitivity of the angle constraint of building block k is:

$$\frac{\partial f_k}{\partial st_k} = \frac{\partial -(sin\theta_k)^2}{\partial sin\theta_k} = -2 * sin\theta_k,\ k = 1, \dots, N.$$

The method of moving asymptotes (MMA) is used as the numerical optimizer, and the Matlab code GCMMA is provided by Dr. Krister Svanberg of KTH.

A design problem

The above problem formulation was investigated using a classic case of a compliance minimization problem with a volume constraint of 0.4.

Figure 2 shows the design domain and boundary conditions of the problem. Displacement is fixed at the left boundary, and a downward force is applied at the center of the right boundary. The design domain is discretized using quadrilateral elements.

Figure 3 shows some known optimized configurations of this design problem from the literature [9], with various dimension ratios of the design boundary.

Fig 2. Design domain and boundary conditions of a TO problem.

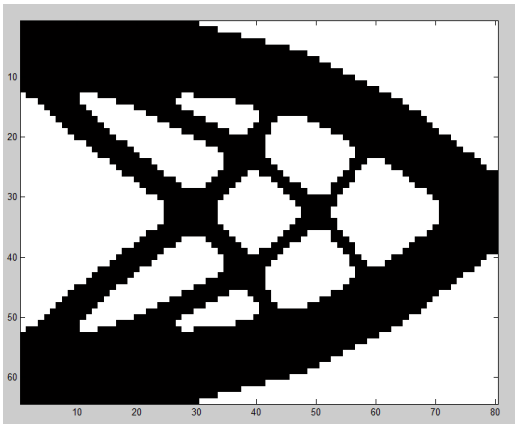

(a)

(b)

Fig 3. Known optimized configurations of the design problem, with dimension ratio length/width: (a) 5:4, (b) 2:1.

Using certain parameters for the optimization, the output structure with a minimum build angle of 40° is shown below in Figure 4:

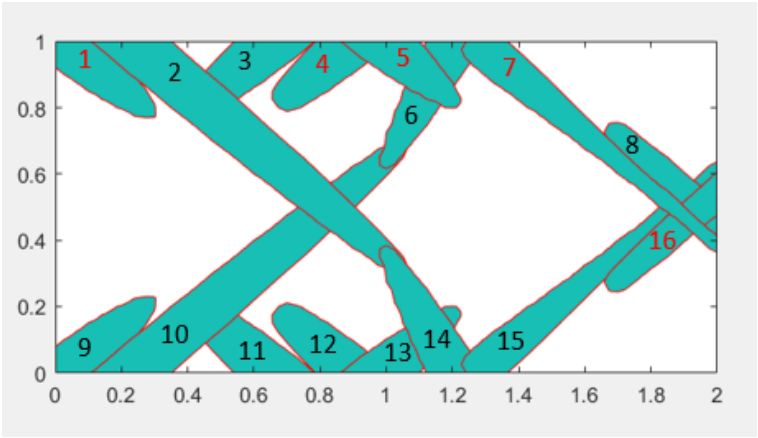

Fig 4. Output structure of the design problem with an overhang angle constraint.

We observe two issues with this output. Firstly, during iterations, the building blocks at the bottom of the structure were trying to form a horizontal bar that resembles the horizontal part at the bottom of the structure without build angle constraints, as shown in Figure 5. This is because a horizontal bottom apparently yields more stiffness to the structure under the specific loading and boundary conditions.

However, the building blocks failed to form a solid horizontal bar due to the definitions of our angle constraints where all building blocks must form an angle larger than the minimum build angle of the machine. The constraints are unnecessary to the building blocks at the bottom of the structure, since they don't need support material at any angle. In other words, the building blocks at the bottom of the design space were over-constrained. We would call it the "over-constraining" issue.

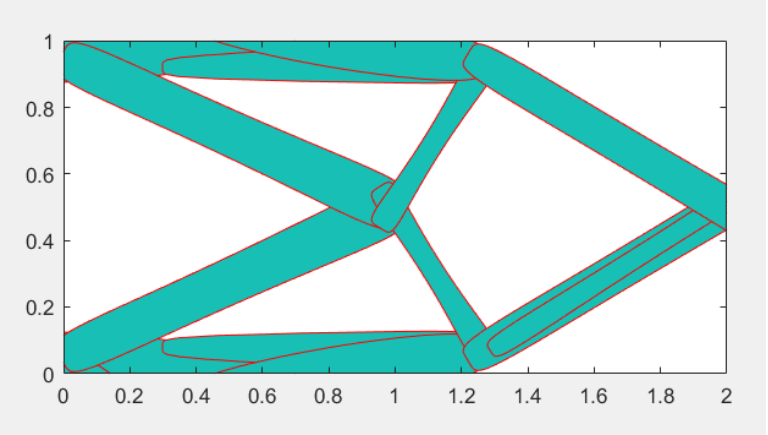

Fig 5. Output structure of the design problem without overhang angle constraint.

Secondly, we can see that this structure is not entirely printable even with minimum angle constraints imposed upon it. Here, building blocks with a red number (1, 4, 5, 7, 16) cannot be printed without support material.

This is because when printing direction is fixed, in addition to the condition that any part of the structure has an angle larger than the minimum build angle, there needs to be material below it, otherwise it would be a piece of material "floating" in the air, such as building blocks 1 and 4, which cannot be printed in a layer by layer fashion. We would call it the "hanging blocks" issue.

Over-Constraining Issue

We used a smoothed Heaviside function $H_\epsilon(x)$ to release the bottom band of design space from the original angle constraints. The new angle constraints are as follows: $f_k(x) = (sin\bar{\theta})^2 * H_\epsilon(\bar{y} - \bar{t}) - (sin\theta_k)^2 \leq 0, k = 1,2,\dots n$, where for any block k, $\bar{y}$ is the mean height of the part of block that is inside the design boundary, and $\bar{t}$ the average thickness of the block.

The smoothed Heaviside function is illustrated in Figure 6 and Equation (1). Its two parameters, ε and α, control the width of the smoothed region, and the constant value of H if x is negative.

In the new angle constraints: When the building block is not at the bottom ($\bar{y} > \bar{t}$), the Heaviside function value is 1 and the angle constraint remains. When building block is close to the bottom design boundary, however, Heaviside function value gradually decreases from 1 to 0, thus the angle constraint becomes relaxed (less strict). This allows building blocks to form smaller angles, or even lie horizontally.

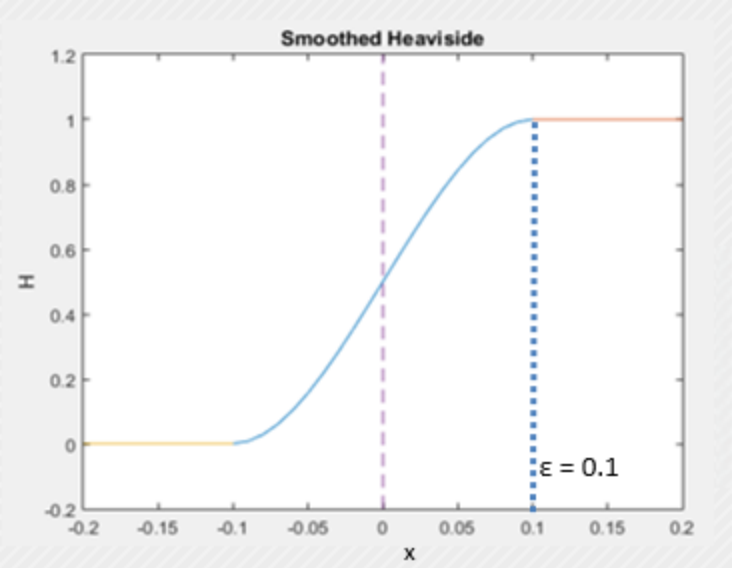

Fig 6. Smoothed Heaviside function.

$$H_\epsilon(x) = \begin{cases} 1, & x > \epsilon \\ \frac{3(1-\alpha)}{4}\left(\frac{x}{\epsilon} - \frac{x^3}{3\epsilon^3}\right) + \frac{(1+\alpha)}{2}, & -\epsilon \le x \le \epsilon \\ \alpha, & x < -\epsilon \end{cases} \quad (1)$$

Figure 7 shows some random intermediate optimization configurations after the new angle constraints were implemented, demonstrating that almost horizontal rods were formed at the bottom to give a stiffer structure.

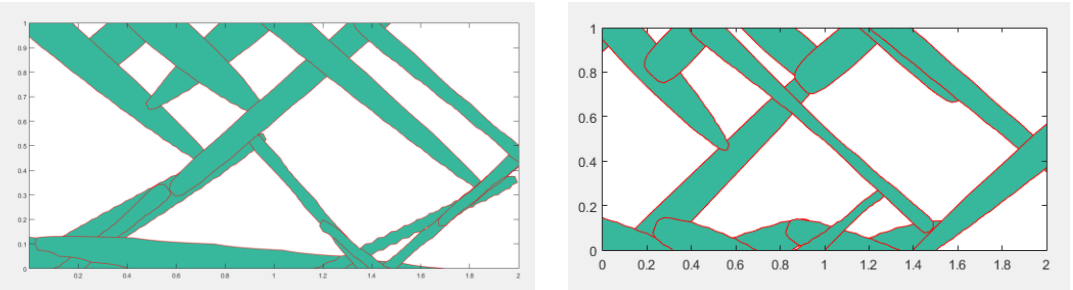

Fig 7. Intermediate configurations with the relaxed version of angle constraints at the bottom layer.

"Hanging Blocks" Issue

Idea: Penalty on nodal densities

To avoid the "floating in the air" situation, our idea is to add a soft constraint: End points of each building block should overlap with at least another building block. End points that are outside of the design boundary are excluded from this constraint. We express it mathematically using the concept of nodal density.

We denote all the end points within the design boundary that are "floating" in the air, thus should be overlapping with other blocks (no matter if they are actually overlapping or not), to be "relevant end points". All relevant end points should satisfy the soft constraint stated above to render a completely printable design.

Procedure

- Identify the relevant end points.
- Calculate the total nodal density H_{tot} at each point.
- Set lower bounds to the total nodal density at each point.
- Define the penalty function and add it in the objective function.
- Compute the sensitivity of the penalty function with respect to design variables.

Step 1. Identify relevant end points

Recall that relevant end points should be within the design boundary and belong to building blocks that do not have material region below.

We divided various scenarios of building blocks' positions and orientations into five categories, shown in Figures 8-12. In each figure, the box represents the design boundary, the line segment is a building block, points E1, E2 indicate its end points, and P_{int} is its intersection point with the boundary.

To identify the end points that would need the overlapping constraint, we analyzed all these different cases which are categorized by positions of the building blocks and their intersections with design boundary. We fixed the print direction to be from bottom up.

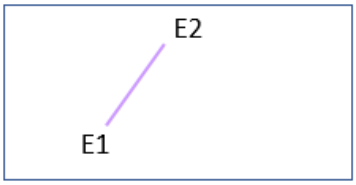

Fig 8. Both end points E1, E2 are relevant end points.

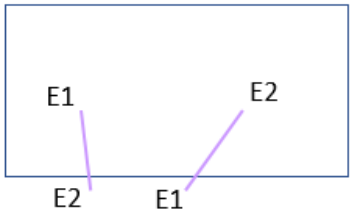

Fig 9. The building blocks do not need support material, so only the end point at the top (i.e. E1 for left block, E2 for right) is relevant end point.

Fig 10. Left block: E2 and P_{int} are relevant end points.
Right block: E1 and P_{int} are relevant end points.

Fig 11. Left block: E2 and P_{int} are relevant end points.
Right block: E1 and P_{int} are relevant end points.

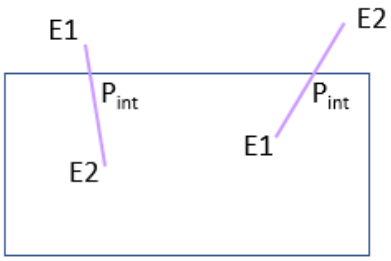

Fig 12. Left block: E2 and P_{int} are relevant end points. Right block: E1 and P_{int} are relevant end points.

Step 2. Level set value -> Nodal density

In brief, nodal density is calculated on each "relevant end point", and is used to express the soft constraints mathematically: $H_{tot} \geq H_{min}$. The number of density values generated at any point equals the number of building blocks. Summing all the density values at a point gives a total density value, or H_{tot}. We would use H_{tot} in the soft constraint.

Each building block generates a 3D level set field across the entire design space that is explicitly described by the following equation (W. Zhang et al.):

$$\phi_i(x,y) = \left(\frac{x'}{L_i}\right)^p + \left(\frac{y'}{f(x')}\right)^p - 1 \tag{2}$$

with

$$\begin{Bmatrix} x' \\ y' \end{Bmatrix} = \begin{bmatrix} \cos\theta_i & \sin\theta_i \\ -\sin\theta_i & \cos\theta_i \end{bmatrix} \begin{Bmatrix} x - x_{0i} \\ y - y_{0i} \end{Bmatrix}$$

An example of the level set contours produced by one building block is shown in Figure 13. Its zero level set contour, i.e. the boundary of the building block, is in red shade.

The morphable components approach then proposes that each building block generates a nodal density field as a function of the level set field. If there are N building blocks, then there are N density values at any point P in the design space, each block producing its own density respectively at point P.

The mathematical relation between the level set value and the density at any point uses again the smoothed Heaviside function (refer to Figure 6):

$$H_\epsilon(\phi) = \begin{cases} 1, \ \phi > \epsilon \\ \dfrac{3(1-\alpha)}{4}\left(\dfrac{\phi}{\epsilon} - \dfrac{\phi^3}{3\epsilon^3}\right) + \dfrac{(1+\alpha)}{2}, \ -\epsilon \leq \phi \leq \epsilon \\ \alpha, \ \phi < -\epsilon \end{cases} \tag{3}$$

In particular, end points of a building block, located on its boundary, have a level set value of zero, i.e. $\phi = 0$. Using the above equations, we know that the point density generated by building block k, at the end points of building block k, is $(1+\alpha)/2$.

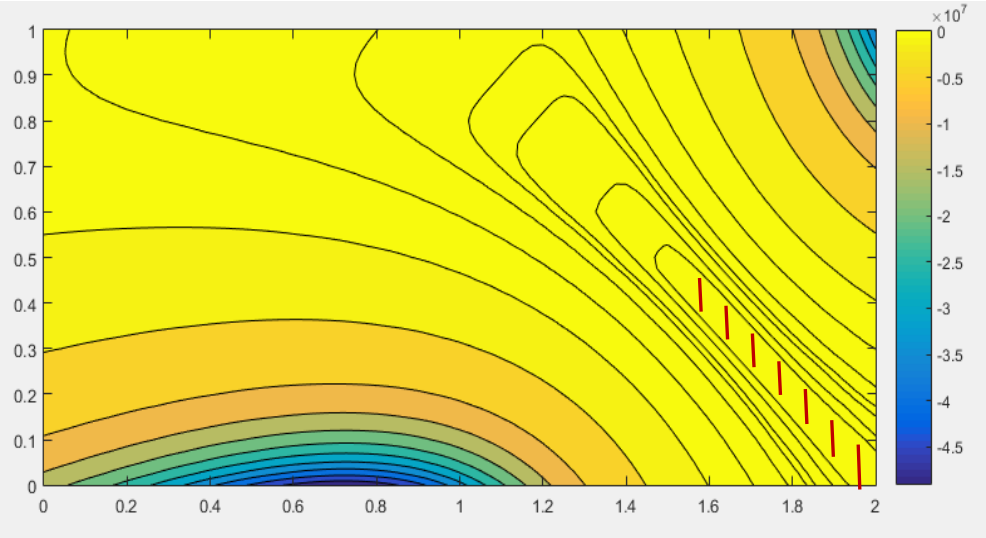

Fig 13. Level set field generated by a building block (in red shade).

Step 3. Determine the lower bounds of the soft constraint.

For an end point of building block A, there are three possible situations illustrated in Figure 14.

i. It happens to be an end point of building block B as well. In this case, the nodal densities H generated by block A and B on the end point are both $(1+\alpha)/2$. Then the total density at this point is $H_{tot} = 1+\alpha$.
ii. It is inside another building block B. From Equation (3), nodal density at this point produced by block B is higher than produced by block A, since it's inside the boundary of B: $H_B > (1+\alpha)/2$. Then the total density at this point is such that: $H_{tot} > 1+\alpha$.
iii. It is not overlapped with any other building block. In this case, nodal density at this point produced by block B is α, a near-zero value. The total density would be $H_{tot} = (1+\alpha)/2$.

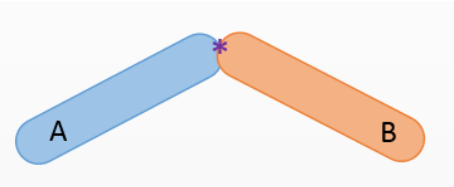

(i) End point "*" of block A is also an end point of block B.

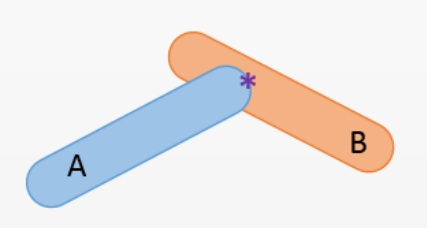

(ii) End point "*" of block A is inside block B.

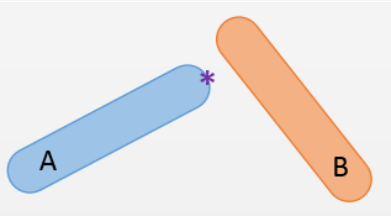

(iii) End point "*" of block A is not overlapped with any other block.

Fig 14. Three possible situations to determine lower bound of the overlapping constraint.

Recall that the soft constraint states that end points of each building block overlap with at least another building block. This means case (i) and (ii) are acceptable, case (iii) is not. Thus we have the soft constraint on any relevant end point to be: $H_{tot} \geq 1+\alpha$.

Step 4. Adding penalty to objective function

One of the ways of solving constrained optimization problems, at least approximately, is by adding a penalty function to the objective function. The idea is to minimize a sequence of unconstrained minimization problems where the infeasibility of the constraints is minimized together with the objective function.

Essentially, we need a penalty term for constraint violation to be a continuous function with the following properties:

- The original problem was to minimize $C = f^T U$.
- The new objective adding the penalty would be: $F = C + \rho * f_{penal}(x)$, where $f_{penal}(x) = 0$ if x is feasible, $f_{penal}(x) > 0$ otherwise.

There are two main types of penalization methods: exterior penalty functions, which impose a penalty for violation of constraints, and interior penalty functions, which impose a penalty for approaching the boundary of an inequality constraint.

Exterior penalty method: The modified objective function is defined as the original objective plus a term for each constraint, which is positive when the current point violates the constraint, and zero otherwise. Thus, optimization needs to start outside the feasible region for the exterior penalty method to work properly, i.e. the initial point needs to be chosen in violation of the constraints.

One of the widely used exterior penalty functions is the quadratic loss function. Recall that our constraint for each relevant end point k is: $H^k_{tot} \geq 1+\alpha$. Here, the quadratic loss function would be:

$$C = U^T KU + \rho * \sum_{k=1}^{numpt} max[0, (1+\alpha) - H^k_{tot}]^2 = \begin{cases} (H^k_{tot} - (1+\alpha))^2, H^k_{tot} < (1+\alpha) \\ 0, H^k_{tot} \geq (1+\alpha) \end{cases}. \quad (4)$$

U^TKU is the structure's compliance, the original objective; ρ (or ρ_{ext}) is the exterior penalty parameter, and numpt is the number of relevant end points.

If a relevant end point k violates the constraint $H^k_{tot} \geq 1+\alpha$, the penalty term related to point k equals $[H^k_{tot} - (1+\alpha)]^2$. If not, zero.

The sensitivity of the penalty term related to end point k that violates the constraint is: $\rho * 2\left(H^k_{tot} - (1+\alpha)\right) * \frac{\partial H^k_{tot}}{\partial \alpha^j_{ii}}$.

One concern about the quadratic loss function is continuity. We need to check if the *max* term in the quadratic loss function in Equation (4) is differentiable, i.e. C^1 continuous, so that sensitivity of the penalty term can be computed.

Following is the penalty term related to any relevant end point:

$$C_{penalty}\left(H^k_{tot}\right) \equiv f(x) = \begin{cases} (x - (1+\alpha))^2, x < (1+\alpha) \\ 0, x \geq (1+\alpha) \end{cases}$$

By differentiating both sides of the equation at $x = 1+\alpha$ (or $H^k_{tot} = 1+\alpha$), we have:

$$f'(1+\alpha) = \lim_{x \to (1+\alpha)^-} \frac{f(x) - f(1+\alpha)}{x - (1+\alpha)} = \frac{(x - (1+\alpha))^2 - 0}{x - (1+\alpha)} = x - (1+\alpha) = 0.$$

$$f'(1+\alpha) = \lim_{x \to (1+\alpha)^+} \frac{f(x) - f(1+\alpha)}{x - (1+\alpha)} = \frac{0 - 0}{x - (1+\alpha)} = 0.$$

We see that the max function is continuous at $H^k_{tot} = 1+\alpha$, $\forall k$. This means the quadratic loss function is C^1 continuous and could be used in the objective function.

Interior penalty method: A second type of penalty function begins with an initial point inside the feasible region, which is why these procedures are called interior penalty functions or "barrier methods". This type of method would not work well once optimization falls out of the feasible region.

There exist several penalty functions of this type; we choose the inverse barrier function, which is as follows in our case:

$C = U^T KU + \mu * \sum_{k=1}^{numpt} \left[\frac{1}{H^k_{tot} - (1+\alpha)}\right]$, where μ (or ρ_{int}) is the interior penalty parameter.

We can see that as long as the constraint $H^k_{tot} \geq 1+\alpha$ stays satisfied, as total density H^k_{tot} approaches its lower bound $(1+\alpha)$, the penalty term becomes infinitely large.

The sensitivity of the penalty term related to relevant end point k is:

$$-\mu * \left(H_{tot}^{k} - (1+\alpha)\right)^{-2} * \frac{\partial H_{tot}^{k}}{\partial a_{ii}^{j}}.$$

Results

We set the minimum build angle to be 30°, 35° and 40°; Figs. 15 and 16 show results for 30° and 35°, respectively.

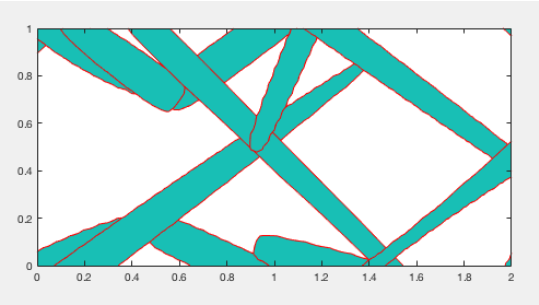

Fig 15. An output structure, with minimum build angle of 30°.

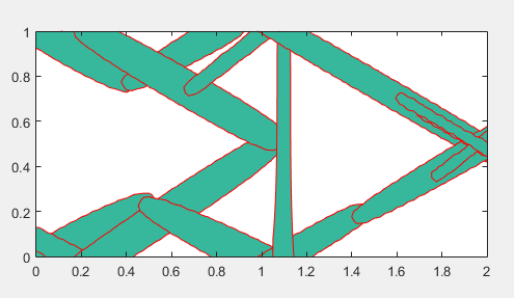

Fig 16. An output structure, with minimum build angle of 35°.

For an optimization with 40 degree overhang angle constraints, convergence usually takes about 500-600 iterations.

There are several parameters involved in the TO framework proposed in this work, for example, the smoothing parameters ε and α in the Heaviside function, and the penalty parameters ρ_{ext}, ρ_{int} for exterior and interior penalty methods, etc.

We observed that the output structure is sensitive to these parameter values. As shown in Figures 17 and 18, the value of ε being .1 and .15 gave these different results. This is something we'll need to investigate further.

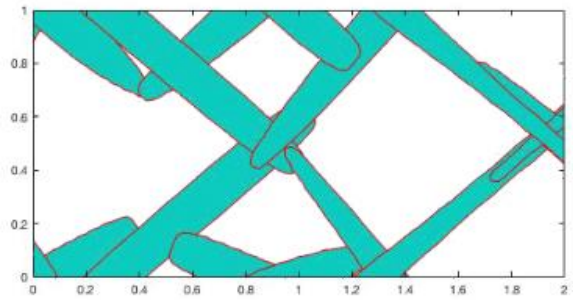

Fig 17. Minimum build angle = 40°
ε = 0.1

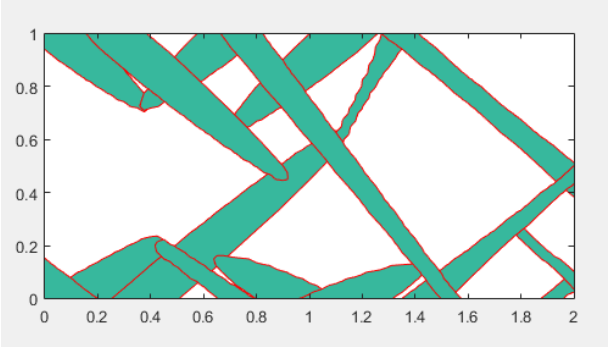

Fig 18. Minimum build angle = 40°
ε = 0.15

Adjusting the various parameters, the "best" result we got for a minimum build angle of 30° is shown in Figure 19 (a). The convergence history is also shown, where we can see the objective value had a few jumps at the start of the calculation, but converged to a minimum value rather smoothly.

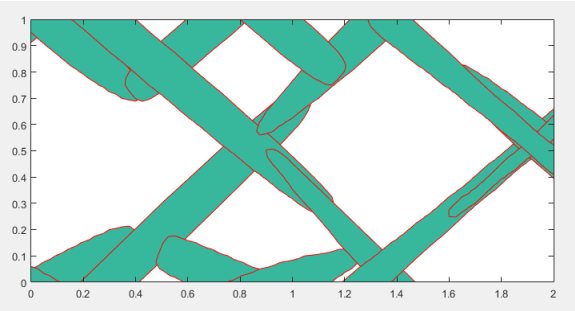

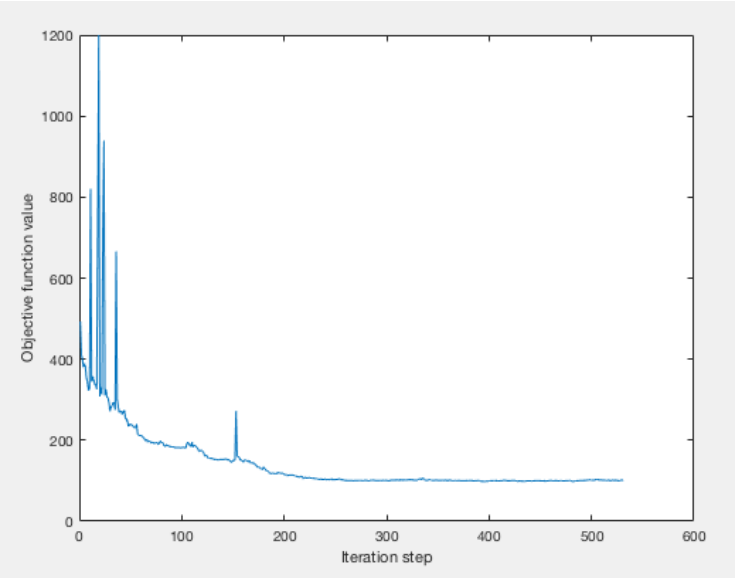

Fig 19. (a) Output structure.
(b) Convergence history plot.
Minimum build angle = 40°;
ε = 0.1; After 200 iterations,
if outeriter > 200
rho_int=.01*0.996^(outeriter-149-1);
rho_ext=2*1.003^(outeriter-149-1);
end

Validation

A simple validation step was done where an output structure with a minimum build angle 45° was built using a Stratasys F170 machine, of which the overhang angle and minimum wall thickness were determined using test parts. We observe from Figure 20 that the output structure was additively manufacturable, i.e. did not require any support material. This validated the first and second objective which are to remove overhangs and to give a geometrically explicit optimization result.

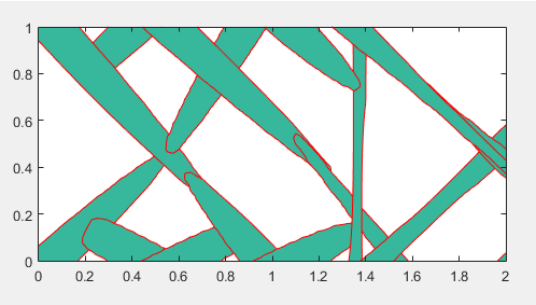

Fig 20. An optimization result.
Minimum build angle = 45°

Fig 21. The corresponding printed part, with no support material, sparse infill.

Conclusions / Future Work

Future Work

We discuss material anisotropy in this section, for we have not completed it yet.

To incorporate 2D orthotropic material properties in topology optimization, we studied 2 cases. In the first, fiber orientation of the entire material region aligns with the design boundary as illustrated in Figure 22. In this case, all we had to do computation wise was to change the element stiffness matrix. In the second case, shown in Figure 23, we assumed each building block has its own fiber orientation, in which case we rotated each element stiffness matrix according to the orientation of the building block it belongs to. We are currently still pursuing this work.

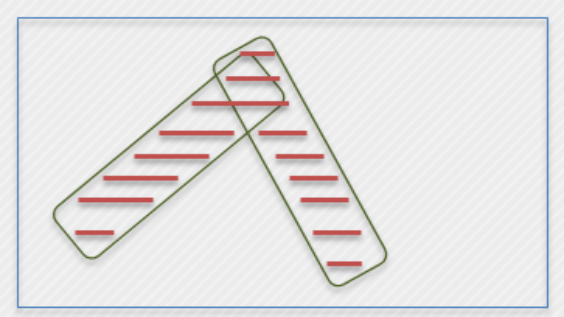

Fig 22. 2D orthotropic case 1: All fiber orientation aligns with design boundary.

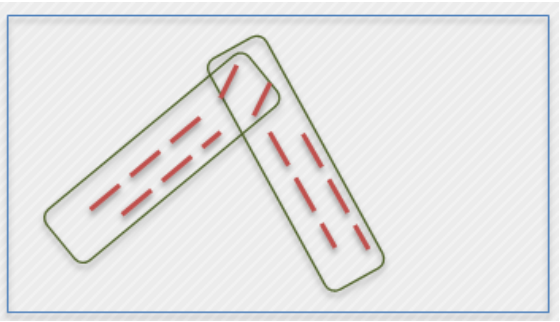

Fig 23. 2D orthotropic case 2: Each building block has its own fiber orientation.

For the first case (Fig. 22), a TO problem was performed with orthotropic properties and compared with results using isotropic properties. Fig. 24 shows the optimized structure using a set of normalized 2D orthotropic material properties extracted from a Stratasys Fortus machine. We observe its difference from the optimization result using isotropic material shown in Fig. 25.

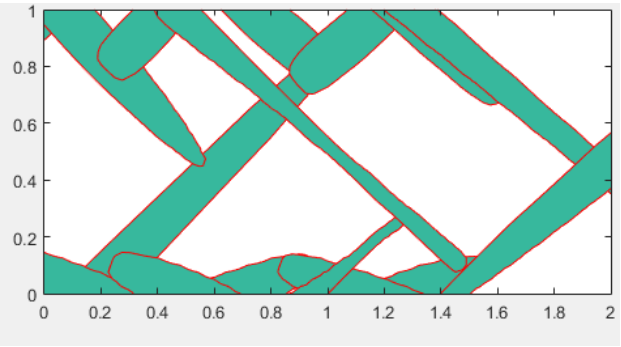

Fig 24. An optimization result, incorporating orthotropic material whose fiber orientation aligns with design boundary.
E1=1, E2=0.85, nu12=0.4, G12=0.25.

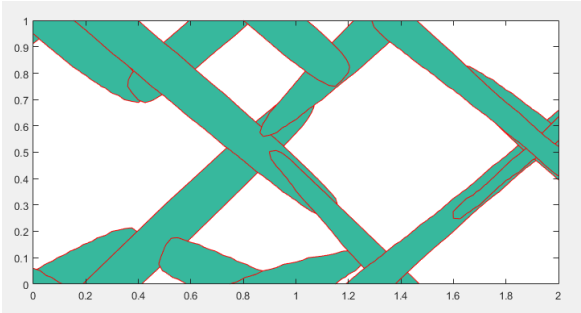

Fig 25. Isotropic material, E=1. Same MMC approach, same optimization parameters as left.

Conclusions

We proposed in this work a moving morphable components-based optimization approach that incorporated additive manufacturing related constraints, such that the following objectives were met:

1. The output structure has explicit boundary and could be easily used for subsequent engineering.
2. Overhangs were removed.
3. Material anisotropy of printed parts was taken into account during optimization.

Acknowledgements

The authors acknowledge partial support for this work from the International Design Centre at the Singapore University of Technology Design, which is funded by the Singapore Ministry of Education.

References

[1] Bendsøe MP, Kikuchi N (1988) Generating optimal topologies in structural design using a homogenization method. Comput Methods Appl Mech Eng 71:197–224

[2] Bendsøe MP (1989) Optimal shape design as a material distribution problem. Struct Multidiscipl Optim 1:193–202

[3] O. Sigmund A 99 line topology optimization code written in Matlab Struct Multidiscip Optim, 21 (2) (2001), pp. 120–127

[4] Wang MY, Wang XM, Guo DM (2003) A level set method for structural topology optimization. Comput Methods Appl Mech Eng 192:227–246

[5] Osher SJ, Sethian JA (1988) Fronts propagating with curvature dependent speed: algorithms based on Hamilton-Jacobi formulations. J Comput Phys 79:12–49

[6] Guo X, Zhang WS, Zhong WL, Doing topology optimization explicitly and geometrically—a new moving morphable components based framework. J Appl Mech (2014) 81:081009.

[7] WS Zhang, J Yuan, J Zhang, X Guo, A new topology optimization approach based on Moving Morphable Components (MMC) and the ersatz material model, Struct Multidisc Optim (2016) 53:1243–1260

[8] X Guo, J Zhou, W Zhang, Z Du, C Liu, Y Liu, Self-supporting structure design in additive manufacturing through explicit topology optimization, Comput. Methods Appl. Mech. Engrg. 323 (2017) 27–63

[9] Otomori M, Yamada T, Izui K, Nishiwaki S (2015) Matlab code for a level set-based topology optimization method using a reaction diffusion equation. Struct Multidiscip Optim 51:1159–1172